

# Subthreshold Low-Transconductance M-CDTA based Low Frequency Current Mode Universal Filter

Varun Bhanoo<sup>1</sup>, Ashmin Gangal<sup>2</sup>, Neeta Pandey<sup>3</sup>

<sup>1</sup>Student, <sup>2</sup>Student, <sup>3</sup>Professor

Department of Electronics and Communication, Delhi Technological University, New Delhi, India

**Abstract** — In this research work, a low transconductance Modified Current Differencing Trans-Conductance Amplifier (M-CDTA) block customized to operate in the sub-threshold region of operation is presented. It is able to achieve a low transconductance value, with the minimum value being  $68.8nA/V$ . As an application, a low frequency current mode universal filter is presented in this manuscript which is used in biomedical signal processing. The structure is composed of two M-CDTA blocks along with two grounded capacitors. The grounded capacitors make the circuit feasible from a fabrication point of view. The circuit has low input as well as high output impedances, which is as desired in a current mode (CM) circuit. The filter also possesses benefits such as electronically tunability of the pole frequencies using bias currents and orthogonal tunability of the pole frequency and the quality factor of the filter. Both the block and the filter are developed on CMOS 180nm technology node. The functionality of the circuit is simulated and verified on Cadence Virtuoso software. The simulation results reveal a good performance of the implemented block as well as the filter.

**Keywords** — CDTA, Low-Transconductance, Subthreshold Regime, Universal Filter.

## I. INTRODUCTION

Recently, in the domain of integrated circuits, a lot of attention has been devoted to various analog building blocks (ABB) due to their enormous implementation in various VLSI applications. Among the existing ABBs, current mode ABB have been more positively acknowledged due to their wider bandwidth, reduced power consumption and increased dynamic range, especially in the area of analog signal processing. CDTA [1] is a current processing ABB and can be advantageously employed in CM circuits as it has all the properties required in a CM block like proper input and output impedances and electronic tunability feature with the help of the bias currents present in the block. The output current in the CDTA block can be controlled using a transconductance value, which is also a really important characteristic of the block. Moreover, filters are an essential part in the field of analog signal processing due to their tremendous

applications and it is desired to obtain all the possible filtered outputs simultaneously from any filter, i.e. universal filters. Thus, a lot of attention has been devoted in the recent past towards obtaining CDTA based universal CM filters. Furthermore, there is also a progressing demand to develop universal filters useful in the domain of biomedical signal processing [2]. Therefore, there is a developing need for filters having extremely low frequencies in the present.

A comprehensive literature survey reveals that many CDTA based universal CM filters [3-19] have been reported previously. To obtain a filter having pole frequency in the sub-hertz range, the previously reported filters [3-19] need to employ capacitors having extremely large values, which is practically not possible from fabrication point of view. Thus, it can be inferred that a universal CM filter having low pole frequencies is not available in the literature and due to the motivation to fulfil this gap, the same has been presented in this manuscript.

This work presents a low-transconductance M-CDTA block operating in subthreshold regime, which is employed in a CM universal filter having low pole frequencies and is thus presented as an application of the presented block. The implemented filter has proper impedances employing grounded capacitances with possibility of electronic tunability of the pole frequency along with orthogonal tunability of the pole frequency and the quality factor.

The organization of the manuscript is in the following manner: Section 2 describes the subthreshold low-transconductance M-CDTA block. Section 3 presents the design, implementation as well as the simulation results of the low frequency CM universal filter employing the low-transconductance M-CDTA block. Conclusions drawn are concluded in Section 4.

## II. THE SUBTHRESHOLD LOW-TRANSCONDUCTANCE M-CDTA

CDTA [1] is a current ABB involving a Current Differencing Unit (CDU) appended with a transconductance amplifier (TA). The M-CDTA i.e. Modified Current Differencing Transconductance

Amplifier is a modified version of the CDTA block, wherein, auxiliary terminals are appended for effective copying of the available output currents in the ABB. Here, additional  $X_+$  terminals are augmented in the block to facilitate copying of currents.

The symbolic representation of the M-CDTA block is depicted in Fig. 1.

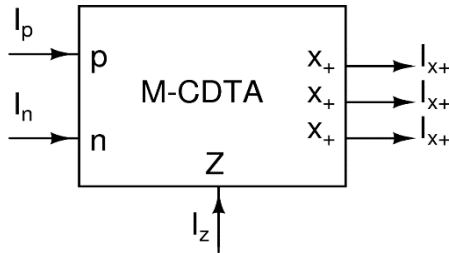


Fig. 1 M-CDTA Symbolic Representation

The functionality of the M-CDTA block is described as follows: the input currents applied at the p and n terminals are subtracted and the subtracted current is then available through the Z terminal. Further, the output current accessible through the X terminals is equal to the voltage produced at the Z terminal multiplied by the transconductance ( $g_m$ ) of the M-CDTA. The functionality of the M-CDTA block can be described using the port relationships provided in (1).

$$\begin{bmatrix} V_p \\ V_n \\ I_z \\ I_{X+} \end{bmatrix} = \begin{bmatrix} 0 & 0 & 0 & 0 \\ 0 & 0 & 0 & 0 \\ 1 & -1 & 0 & 0 \\ 0 & 0 & g_m & 0 \end{bmatrix} \begin{bmatrix} I_p \\ I_n \\ V_z \\ I_{X+} \end{bmatrix} \quad (1)$$

The CMOS implementation of the M-CDTA block is described in Fig. 2. The CMOS implementation of the MCDTA block present in [10] is adapted and redesigned to incorporate the required additional terminals. Also, the M-CDTA block is customized to operate in the subthreshold region of operation by employing low power supply ( $V_{DD}$  and  $V_{SS}$ ) near the threshold voltage of the transistors and also employing low bias currents ( $I_1$ ,  $I_2$  and  $I_3$ ).

On routine analysis, the relation between the output current ( $I_{X+}$ ) of the M-CDTA block with the voltage at the Z terminal ( $V_z$ ) is expressed in (2) where  $I_{bias}=I_3$  and relation between  $g_m$  of the block with the bias current can be expressed in (3). In (2) and (3),  $\kappa$  represents the exponential coefficient in the subthreshold region,  $V_t$  represents the thermal voltage and  $n$  represents the ideality factor of the semiconductor.

$$I_{X+} = I_{bias} \tanh \frac{\kappa V_z}{V_t} \quad (2)$$

$$g_m = \frac{I_{bias}}{2nV_t} \quad (3)$$

The relation between the  $g_m$  and bias current in case of saturation region of operation of transistors, is expressed in (4).

$$g_{m_{saturation}} = \sqrt{2 \mu_n C_{ox} \left(\frac{W}{L}\right) I_{bias}} \quad (4)$$

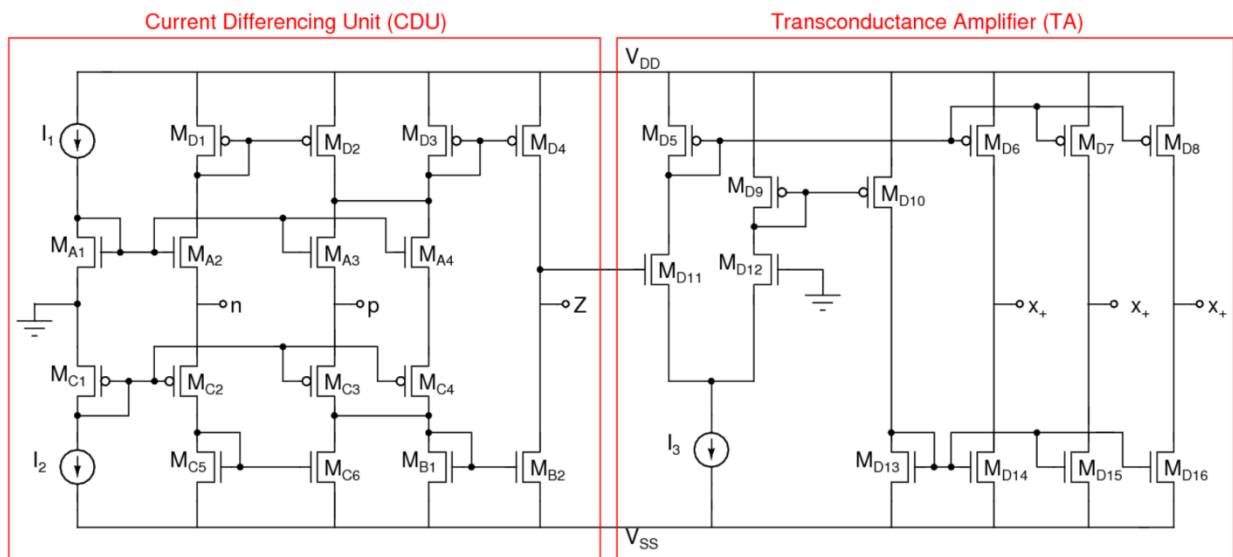


Fig. 2 CMOS Implementation of the subthreshold low-transconductance M-CDTA block

From (3) and (4), it can be noted that with same bias currents (usually in the range of  $\mu A$ - $nA$ ), lower

transconductance can be obtained using subthreshold region of operation due to direct relationship of the

$g_m$  with the bias current. Thus, the transconductance values of the CDTA block, usually operated in the saturation region of operation, are in the range of microsiemens ( $\mu S$ ), whereas, when being operated in the subthreshold region of operation, the transconductance values of the CDTA block reduces drastically to the nanosiemens (nS) range. Therefore, as the pole frequencies in most filters are dependent on the transconductance values of the ABB, it is preferred to reduce the transconductance to obtain low pole frequencies, which, which is possible by operating the ABB in the subthreshold regime.

To verify the functionality of the subthreshold low-transconductance M-CDTA on block, characterization of the block is performed using Cadence Virtuoso simulations for 180nm technology. To ensure subthreshold operation, the aspect ratios of the transistors are selected as shown in Table 1. The power supply voltages ( $V_{DD}$  and  $V_{SS}$ ) are set to be 0.3V and -0.3V and the bias currents as  $I_1=I_2=I_3=5nA$ .

**TABLE I. ASPECT RATIO OF THE TRANSISTORS**

Transistors	Aspect Ratios (W/L)
$M_{A1}-M_{A4}$	600nm/500nm
$M_{B1}-M_{B2}$	$2\mu m/1.5\mu m$
$M_{C1}-M_{C6}$	$2\mu m/500nm$
$M_{D1}-M_{D16}$	700nm/500nm

Current transfer from p to Z and n to Z; p to  $X_+$  and n to  $X_+$  terminals is depicted in the form of current transfer characteristics with respect to frequency in Figures 3 and 4 respectively. Fig. 5 illustrates the variation in  $g_m$  with frequency with various values of bias current ( $I_3$ ).

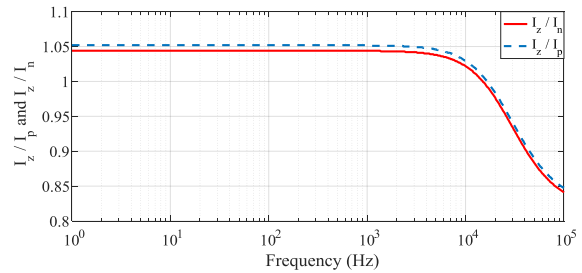


Fig. 3 Current transfer characteristics from p to Z and n to Z terminals

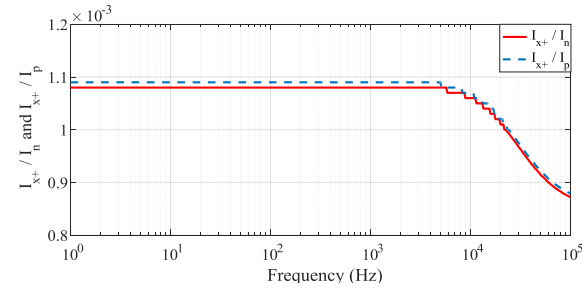


Fig. 4 Current transfer characteristics from p to  $X_+$  and n to  $X_+$  terminals

Impedance seen from various terminals of the block is also calculated and the impedance seen from p & n, Z &  $X_+$  terminals with frequency is shown in Fig. 6. As the M-CDTA block is a current processing block, impedances at the I/O terminals are expected to be low/high and the same has been obtained in the simulation analysis. Thus, the block has proper impedances.

The simulation results of the subthreshold low-transconductance M-CDTA block is provided in Table 2.

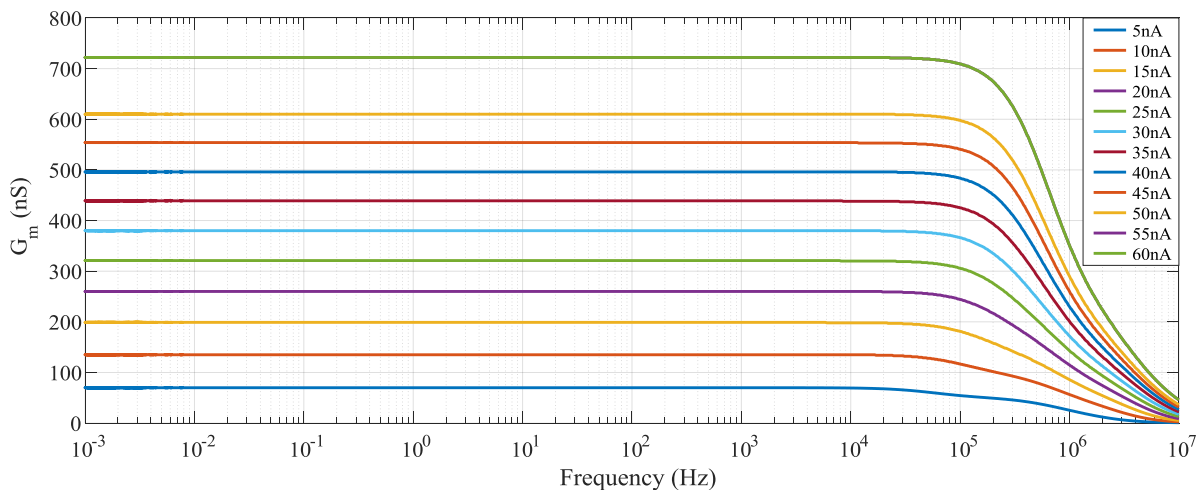
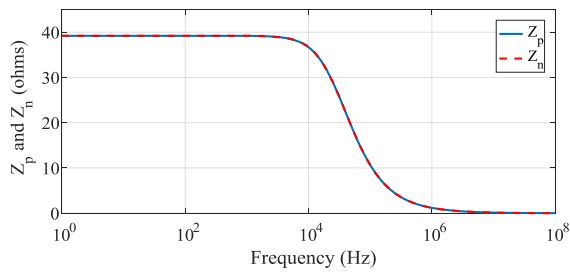
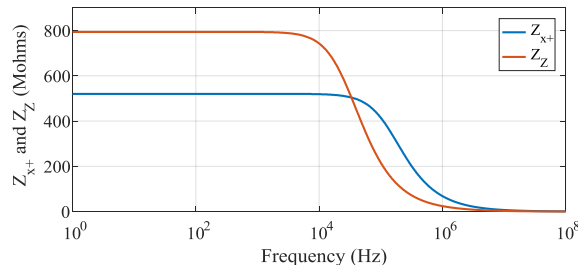


Fig. 5 Variation in  $g_m$  with frequency for various bias currents



(a)



(b)

Fig. 6 Impedance at (a) p, n (b) Z, X<sub>+</sub> terminals

### III. APPLICATION

The functionality of the subthreshold low-transconductance M-CDTA block is verified using a low frequency universal filter [4] described in Fig. 7. The universal filter consists of two active M-CDTA blocks and two passive grounded capacitors. It is a Multiple Input Single Output (MISO) filter. The general transfer function of the filter can be presented as expressed in equation (5).

$$I_{out} = \frac{s \frac{g_m}{c_1} I_1 + \frac{g_m^2}{c_1 c_2} I_2 + \left( s^2 + \frac{g_m}{c_1} s + \frac{g_m^2}{c_1 c_2} \right) I_3}{s^2 + \frac{g_m}{c_1} s + \frac{g_m^2}{c_1 c_2}} \quad (5)$$

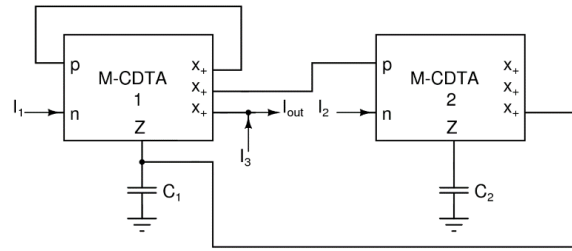


Fig. 7 Low Frequency Filter [4]

An in-depth exploration of the general transfer function shows that the filter is capable of providing all Low pass (LP), High Pass (HP), Band Pass (BP), Band Reject (BR) and All pass (AP) responses. The different conditions which result in various filtered responses along with their transfer functions are described below:

1. For LP response, required input current combinations are:  $I_1=0, I_2=I_{in}, I_3=0$  and its transfer function is expressed in (6).

$$\frac{I_{out}}{I_{in}} = \frac{g_m^2}{c_1 c_2 D(s)} \quad (6)$$

2. For HP response, required input current combinations are:  $I_1=-I_{in}, I_2=-I_{in}, I_3=I_{in}$  and its transfer function is expressed in (7).

$$\frac{I_{out}}{I_{in}} = \frac{s^2}{D(s)} \quad (7)$$

3. For BP response, required input current combinations are:  $I_1=I_{in}, I_2=0, I_3=0$  and its transfer function is expressed in (8).

$$\frac{I_{out}}{I_{in}} = \frac{g_m s}{c_1 D(s)} \quad (8)$$

TABLE II. SIMULATION RESULTS

Parameter	Value	Condition
Supply Voltage	±0.3V	-
Process Parameters	180nm	-
Bias Currents ( $I_1, I_2, I_3$ )	5nA, 5nA, 5nA	-
Parasitic Gains ( $\alpha_p, \alpha_n$ )	1.051, 1.043	-
3-dB Bandwidth	$I_z / I_p$	592.30 kHz Z terminal grounded
	$I_z / I_n$	546.744 kHz Z terminal grounded
	$I_{x+} / I_p$	567.238 kHz Z terminal grounded
	$I_{x+} / I_n$	527.481 kHz $R_z = 1k\Omega$ for 59.24 dB gain
	$I_{x+} / V_z$	4.489 MHz $R_z = 1k\Omega$ for 59.30 dB gain
Transconductance Gain ( $g_m$ )	68.9 nS	$X_+$ terminals grounded
Input impedance at p and n ( $Z_p$ and $Z_n$ )	39.2 $\Omega$	Z and $X_+$ terminals grounded
Output Impedance at Z ( $Z_z$ )	794.383 M $\Omega$	p, n and $X_+$ terminals grounded
Output Impedance at $X_+$ ( $Z_{x+}$ )	520.328 M $\Omega$	p, n and Z terminals grounded

4. For BR response, required input current combinations are:  $I_1=-I_{in}$ ,  $I_2=0$ ,  $I_3=I_{in}$  and its transfer function is expressed in (9).

$$\frac{I_{out}}{I_{in}} = \frac{s^2 + \frac{g_m^2}{C_1 C_2}}{D(s)} \quad (9)$$

5. For AP response, required input current combinations are:  $I_1=-2I_{in}$ ,  $I_2=0$ ,  $I_3=I_{in}$  and its transfer function is expressed in (10).

$$\frac{I_{out}}{I_{in}} = \frac{s^2 - \frac{g_m}{C_1}s + \frac{g_m^2}{C_1 C_2}}{D(s)} \quad (10)$$

In equations (6)-(10),  $D(s)$  is described in (11).

$$D(s) = s^2 + \frac{g_m}{C_1}s + \frac{g_m^2}{C_1 C_2} \quad (11)$$

The pole frequency ( $\omega_o$ ), bandwidth ( $BW$ ) and the quality factor ( $Q_o$ ) of the filter are described in (12), (13) and (14) respectively.

$$\omega_o = \frac{g_m}{\sqrt{C_1 C_2}} \quad (12)$$

$$BW = \frac{g_m}{C_1} \quad (13)$$

$$Q_o = \sqrt{\frac{C_1}{C_2}} \quad (14)$$

From (12), it can be concluded that to reduce the pole frequency we have to either reduce the transconductance of the TA stage of the M-CDTA block or to employ large-valued capacitances. Increasing the capacitance is not a preferred approach, due to the increase in the chip area during the fabrication process. Hence, this paper aims to reduce the transconductance of the TA stage. This reduction in  $g_m$  is achieved by biasing the M-CDTA block to obtain subthreshold region of operation for all the transistors, which reduces  $g_m$  drastically as explained in Section 2. The electronic tunability of the pole frequencies is possible by changing  $g_m$ , which can be accomplished by varying the bias currents in the M-CDTA block.

All the simulations are performed on Cadence Virtuoso 180nm Technology Node. Table 1 indicates the aspect ratios of the transistors of the M-CDTA block. The power supply voltage and the bias currents are selected as:  $V_{DD}=0.3V$ ,  $V_{SS}=-0.3V$  and  $I_1=I_2=I_3=5nA$  respectively.

The frequency domain analysis of the filter is performed using the capacitance values as  $C_1=1nF$ ,  $C_2=2nF$ , to obtain the value of  $Q_o$  as 0.707. The simulation results of LP, HP and BP response is shown in Fig. 8. The simulation result of the BR response is depicted in Fig. 9. The simulated magnitude and phase responses of the AP filter is shown in Fig. 10. The simulated stand close to the theoretical predictions proving the effectiveness of the block with the filter.

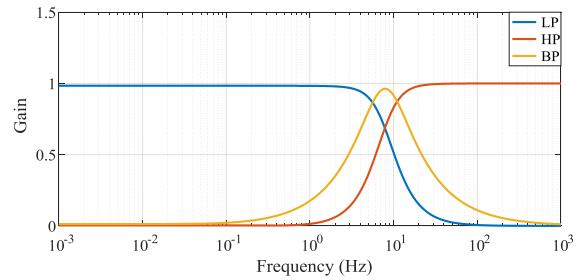


Fig. 8 LP, HP and BP Response

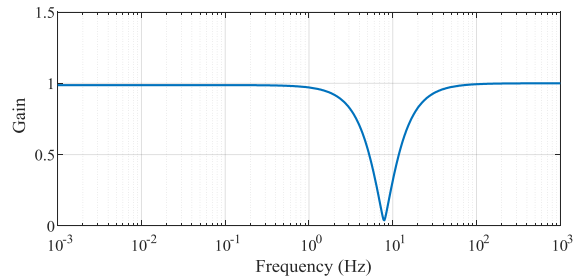


Fig. 9 BR Response

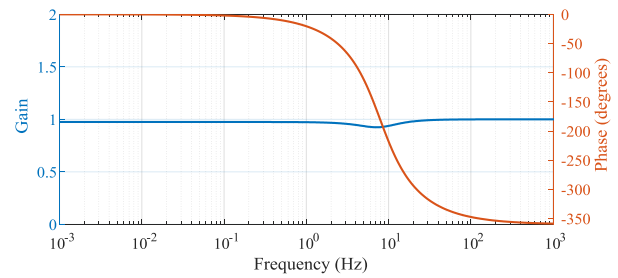


Fig. 10 AP Response

To check the resilience of the filter against noise, noise analysis is performed. The input referred noise is depicted in Fig. 11. It can be seen from the simulation result, that the maximum noise is 248 nV/√Hz and thus, it can be inferred that the filter is insensitive towards noise.

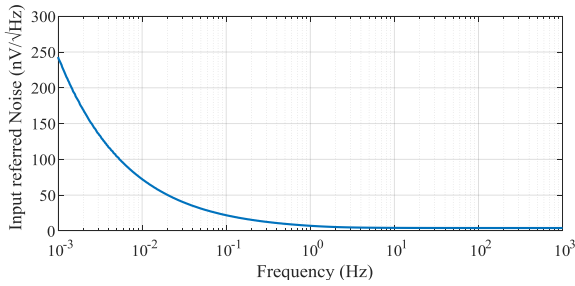


Fig. 11 Noise Analysis

The electronic tunability of the filter is examined using the different values of the bias current  $I_3$  ranging from 5nA to 60nA in steps of 5nA. BP is selected to illustrate this feature using capacitance values as  $C_1=1nF$ ,  $C_2=2nF$ . The response is shown in Fig. 12. It is observed that different bias currents lead to different pole frequencies leading to electronic tunability of the pole frequencies in the circuit.

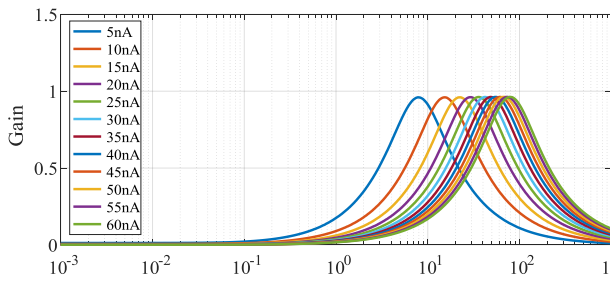


Fig. 12 Electronic tunability using bias current ( $I_3$ )

The  $\omega_o$  and  $Q_o$  are capable of orthogonal tunability using the capacitances:  $C_1$  and  $C_2$ . Variation in pole frequency with constant quality factor can be achieved by maintaining same  $C_1/C_2$  when the product  $C_1C_2$  changes. Whereas, variation in quality factor with constant pole frequency can be achieved by maintaining constant product  $C_1C_2$  when the quotient  $C_1/C_2$  changes. The simulation results for both of these cases using BP response is shown in Fig. 13 and the capacitance values required along with the obtained  $\omega_o$  and  $Q_o$  of both of the cases are mentioned in Tables 3 and 4. It can be inferred from the simulation results that it is possible to orthogonally tune the pole frequency and the quality factor as per the requirement.

TABLE III. VARIABLE  $Q_o$  WITH CONSTANT  $\omega_o$ : SIMULATION RESULTS

Capacitance		Quality Factor ( $Q_o$ )
$C_1$	$C_2$	( $\omega_o=7.7$ Hz)
16nF	1nF	4
8nF	2nF	2
4nF	4nF	1
8nF	2nF	0.5
16nF	1nF	0.25

TABLE IV. VARIABLE  $\omega_o$  WITH CONSTANT  $Q_o$ : SIMULATION RESULTS

Capacitance		Pole Frequency
$C_1$	$C_2$ (nF)	( $Q_o=0.707$ )
1nF	2nF	7.7 Hz
2nF	4nF	3.89 Hz
3nF	6nF	2.59 Hz
4nF	8nF	1.94 Hz
5nF	10nF	1.55 Hz
6nF	12nF	1.29 Hz
7nF	14nF	1.11 Hz

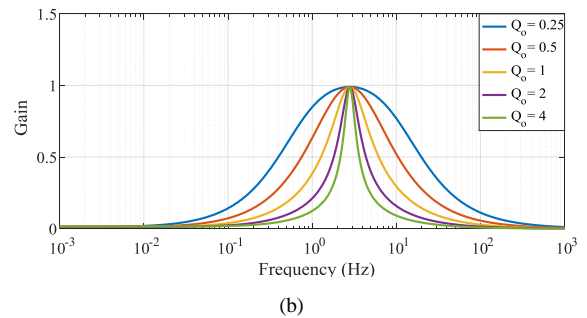
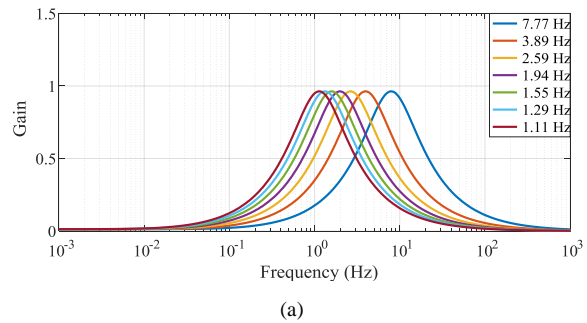


Fig. 13 Orthogonal Tunability of (a)  $\omega_o$  with  $Q_o$  (b)  $Q_o$  with  $\omega_o$

The capacitors once fabricated, are susceptible to mismatches, leading to slight variations in their capacitance values from their ideal values. This mismatch is studied by Monte Carlo simulations. The histogram after 40 runs for  $\pm 5\%$  gaussian variation in all capacitances is shown in Fig. 14. It is inferred from the histogram that the spread in the pole frequency is observed to be 9.96%.

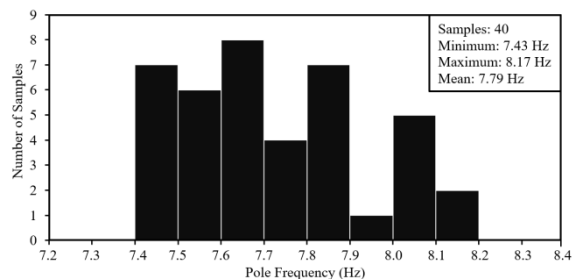


Fig. 14 Monte Carlo Analysis

#### IV. CONCLUSION

This paper presents a low transconductance M-CDTA block customized to operate in the sub-threshold region of operation achieving a low transconductance value i.e. 68.9nA/V. It is further verified using a universal CM low frequency filter useful in many biomedical applications. The low frequency filter has a low pole frequency of 7.77Hz and also, has a number of advantages such as, all the passive components of the filter are grounded which makes it appropriate for fabrication along with proper input and output impedances. The pole frequency is electronically tunable with the bias currents. The mismatch in the passive components are verified using Monte Carlo simulations which gives a maximum 9.96% variation in the pole frequency. Also, using noise analysis, it can be inferred that the filter is insensitive towards noise. Further, it also has the feature of orthogonal tunability of  $\omega_o$  and  $Q_o$ .

#### REFERENCES

- [1] D. Biolek, "CDTA-building block for current-mode analog signal processing," In Proceedings of the ECCTD, vol. 3, pp. 397-400, 2003.
- [2] A. A. Fedotov, "Selection of parameters of bandpass filtering of the ECG signal for heart rhythm monitoring systems," Biomedical Engineering, vol. 50, no. 2, pp. 114-118, 2016.
- [3] P. Prommee, T. Pattanatadapong, K. Angkeaw and M. Somdunyanok, "Low-Input Impedance CMOS MO-CDTA and its Universal Filter Application," In ITC-CSCC, p. 931, 2010.
- [4] J. Jin and C. Wang, "Current-mode universal filter and quadrature oscillator using CDTAs," Turkish Journal of Electrical Engineering & Computer Sciences, vol. 22, no. 2, pp. 276-286, 2014.
- [5] M. Somdunyanok, M. Siripruchyanun and P. Prommee, "CMOS multiple-output CDTA and its Applications," In Proc. 1st Int. Conf. Technical Education, pp. 184-187, 2009.
- [6] T. Dumawipata, W. Tangsrirat and W. Surakampontorn, "Cascadable current-mode multifunction filter with two inputs and three outputs using CDTAs," In 6th International Conference on Information, Communications & Signal Processing, pp. 1-4, 2007.
- [7] T. Dumawipata, W. Tangsrirat and W. Surakampontorn, "Current-mode universal filter with four inputs and one output using CDTAs," In 2006 IEEE Asia Pacific Conference on Circuits and Systems, pp. 892-895, 2006.
- [8] D. Biolek and V. Biolková, "CDTA-C current-mode universal 2nd-order filter," In Proceedings of the 5th WSEAS International Conference on Applied Informatics and Communications, pp. 411-414, 2005.
- [9] M. Kumngern and K. Dejhan, "Current-mode multifunction biquad filter with three inputs five outputs using ZC-CDTAs," In 2012 Second International Conference on Digital Information and Communication Technology and its Applications (DICTAP), pp. 309-313, 2012.
- [10] M. Kumngern, K. Khwama and S. Junnapiya, "Three-input single-output current-mode universal filter using a MCDTA," In 2013 Eleventh International Conference on ICT and Knowledge Engineering, pp. 1-4, 2013.
- [11] N.A. Shah, M. Quadri and S.Z. Iqbal, "Realization of CDTA based current-mode universal filter," Indian Journal of Pure and Applied Physics, vol. 46, pp. 283-285, 2008.
- [12] J. Jin, "Resistorless active SIMO universal filter and four-phase quadrature oscillator," Arabian Journal for Science and Engineering, vol. 39, no. 5, pp. 3887-3894, 2014.
- [13] A.R. Nasir and S.N. Ahmad, "Single CDTA based current-mode universal filter with grounded capacitors," International Journal of Electronics Engineering, 4, pp. 73-75, 2012.
- [14] W. Tangsrirat, T. Dumawipata and W. Surakampontorn, "Multiple-input single-output current-mode multifunction filter using current differencing transconductance amplifiers," AEU-International Journal of Electronics and Communications, vol. 61, no. 4, pp. 209-214, 2007.
- [15] D. Biolek and V. Biolkova, "Universal biquads using CDTA elements for cascade filter design," Proceeding of the CSCC, pp. 232-236, 2003.
- [16] D. Prasad, D.R. Bhaskar and A.K. Singh, "Universal current-mode biquad filter using dual output current differencing transconductance amplifier," AEU-International Journal of Electronics and Communications, vol. 63, no. 6, pp. 497-501, 2009.
- [17] A. Uygur, H. Kuntman and A. Zeki, "Multi-input multi-output CDTA-based KHN filter," In Proc. of ELECO: The 4th International Conference on Electrical and Electronics, pp. 46-50, 2005.
- [18] S. Summart and C. Thongsopa, "CDTAs Based Current-Mode Universal Biquad Filters with Orthogonal Control of Quality Factor and Pole Frequency," In Advanced Materials Research, vol. 787, pp. 501-507, 2013.
- [19] M. Kumngern and U. Torteanchai, "Four-input four-output current-mode multifunction filter using CDTAs," In 2017 2nd International conferences on Information Technology, Information Systems and Electrical Engineering (ICITISEE), pp. 436-439, 2017.